

## Supporting Information

### **Palladium Cube with Pt Shell Deposition for Localized Surface Plasmon Resonance Enhanced Photodynamic and Photothermal Therapy of Hypoxic Tumor**

*Wenxiang Gu<sup>1,2</sup>, Zhiyuan Hua<sup>2</sup>, Zheng Li<sup>1,2</sup>, Zhiheng Cai<sup>1</sup>, Wandong Wang<sup>1</sup>, Kaijin Guo<sup>2</sup>, Feng Yuan<sup>2</sup>, Fenglei Gao<sup>1,\*</sup> and Hongliang Chen<sup>1,2,\*</sup>*

<sup>1</sup>Jiangsu Key Laboratory of New Drug Research and Clinical Pharmacy, Xuzhou Medical University, Jiangsu 221002, People's Republic of China.

<sup>2</sup>Department of Orthopedics, Affiliated Hospital of Xuzhou Medical University, Jiangsu 221002, People's Republic of China.

\*Corresponding authors: jsxzgfl@sina.com (F. Gao), xzchenhl@sina.com (H. Chen).

## Contents

<b>Materials and Reagents</b> .....	S3
<b>Instruments</b> .....	S3
<b>Preparation of Pd Cubic Seeds</b> .....	S3
<b>Synthesis of Pd@Pt Nanocubes</b> .....	S4
<b>Surface Modification of Pd@Pt Nanocubes</b> .....	S4
<b>Determination of Oxygen generation in vivo</b> .....	S4
<b>Fluorescence spectra (Figure S1)</b> .....	S5
<b>Temperature variation (Figure S2)</b> .....	S5
<b>Plot of Cooling Time (Figure S3)</b> .....	S6
<b>Cell viabilities (Figure S4)</b> .....	S7
<b>In vivo ultrasound images (Figure S5)</b> .....	S7
<b>H&amp;E staining images (Figure S6)</b> .....	S8
<b>Blood levels of Pd@Pt-PEG (Figure S7)</b> .....	S8
<b>Biodistribution of Pd@Pt-PEG (Figure S8)</b> .....	S9
<b>Accumulated Pd contents in urine and feces (Figure S9)</b> .....	S9
<b>Serum biochemistry and hematology analysis (Figure S10)</b> .....	S10

**Materials and Reagents.** Sodium tetrachloropalladate ( $\text{Na}_2\text{PdCl}_4$ ), sodium hexachloroplatinate (IV) hexahydrate ( $\text{Na}_2\text{PtCl}_6 \cdot 6\text{H}_2\text{O}$ ), polyvinylpyrrolidone (PVP, MW=10,000), fluorescein PEG thiol(FITC-PEG-SH, MW=5000) were obtained from Aladdin Chemistry, Co., Ltd. Absolute ethanol, ascorbic acid (AA), potassium bromide (KBr), ethylene glycol (EG) and hydrogen peroxide ( $\text{H}_2\text{O}_2$ ) were purchased from Sinopharm Chemical Reagent Co., Ltd. 1,3-diphenylisobenzofuran (DPBF), and 2',7'-dichlorodihydrofluorescein diacetate (DCFH-DA) were purchased from Sigma-Aldrich. Cell counting kit assay (CCK-8), Live-Dead Cell Staining Kit and phosphate-buffered saline (PBS) powder were obtained from Beyotime Institute of Biotechnology (Shanghai, China). N-acetylcysteine (NAC) was purchased from Solarbio Science Technology Co., Ltd. The LM8 and L929 cell lines were obtained from the Cell Bank of the Chinese Academy of Sciences (Shanghai, China). In this work, all of the reagents were obtained from commercial suppliers and used as received.

**Instruments.** The morphology and structure of as-prepared nanoparticles were characterized using transmission electron microscopy imaging (FEI Tecnai G2 Spirit Twin, Holland). The scanning transmission electron microscopy (STEM) and elemental mapping images were obtained to the elemental composition. X-ray photoelectron spectroscopy (XPS) was evaluated using X-ray photoelectron spectrometer (Thermo Scientific Escalab 250Xi). The Fourier-transform infrared spectroscopy (FTIR) spectrum was recorded on a FTIR-8400S spectrometer (Shimadzu, Japan). UV-vis absorption spectra were recorded by an Evolution 220 UV-Visible Spectrophotometer (Thermo Fisher Scientific). The fluorescence emission spectra were measured on a F4600 spectrofluorometer (Hitachi, Japan). Flow cytometry was carried out by using BD LSRFortessa flow cytometer. The hydrodynamic diameters were determined using a Malvern ZetaSizer Nano-ZS instrument.

**Preparation of Pd Cubic Seeds.** The Pd cubic seeds were fabricated according to a previously reported method. Simply, 105 mg of PVP (MW=10,000), 60 mg of AA, 600 mg of KBr, and 8 mL

of deionized (DI) water were added in a 50 mL vial and preheated at 80 °C for 10 min in an oil bath under continuous magnetic stirring. 57 mg of Na<sub>2</sub>PdCl<sub>4</sub> were dissolved in 3 mL of DI water and then introduced into the preheated solution. The vial was capped and maintained at 80 °C for an additional 3 h. Finally, the samples were collected by centrifugation, washed three times with DI water, and redispersed in 11 mL of DI water for further application.

**Synthesis of Pd@Pt Nanocubes.** In a standard procedure, 1.0 mL of the Pd cubic suspension prepared above, 66.6 mg of PVP, 100 mg of AA, 54 mg of KBr and 12 mL of EG were mixed together in a 50 mL three-neck flask and preheated at 110 °C for 1 h. The reaction temperature was then quickly ramped to 200 °C within 10 min. The deposition of Pt atomic layers was initiated by injecting 12 mL of Na<sub>2</sub>PtCl<sub>6</sub>•6H<sub>2</sub>O solution in EG (0.25 mg/mL) into the reaction solution at a relatively slow rate of 4.0 mL/h. After the injection of all the precursor solution, the reaction solution was kept at 200 °C for another 1 h. The final samples were collected by centrifugation, washed twice with ethanol and three times with DI water, and redispersed in DI water.

**Surface Modification of Pd@Pt Nanocubes.** In order to conjugating with FITC-PEG-SH, the freshly prepared Pd@Pt nanocubes were purified by centrifugation at 10000 rpm for 20 minutes and re-dispersed in an aqueous solution of FITC-PEG-SH (1.0 mL, 0.10 mg/mL). The mixture was ultrasonicated for 10 min and then stirred for over 12 hours at room temperature. To remove the unused FITC-PEG-SH, the product was centrifuged at 10,000 rpm, and then rinsed with deionized water three times. Finally, the Pd@Pt-PEG were redispersed in water or PBS for further use.

**Determination of Oxygen generation in vivo.** For in vivo oxygen generation, 0.1 mL of Pd@Pt-PEG suspension (2 mg/mL) was injected intravenously into the LM8 tumor-bearing mice. The B-mode US images were captured before injection and at specific times (30, 60, and 120 min post-injection) through the US system. Hyper echoes were detected, and post-gray scale values of US

intensity in the treatment groups were recorded using software GrayVal 1.0.

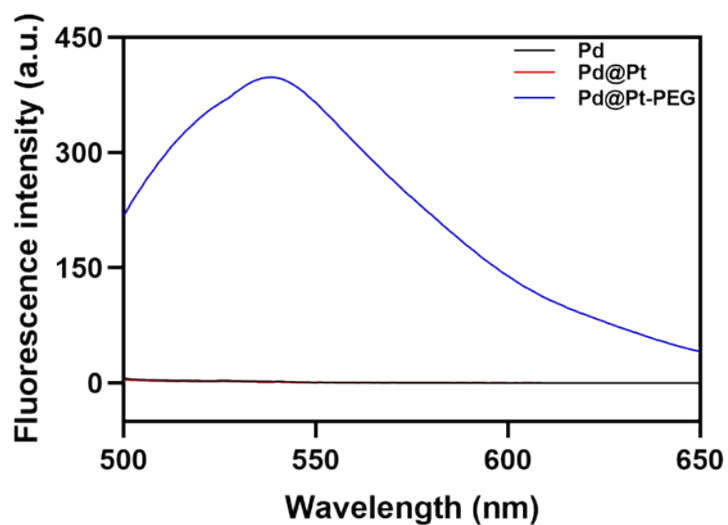


**Figure S1.** The fluorescence spectra of Pd cubes, Pd@Pt cubes, and Pd@Pt-PEG.

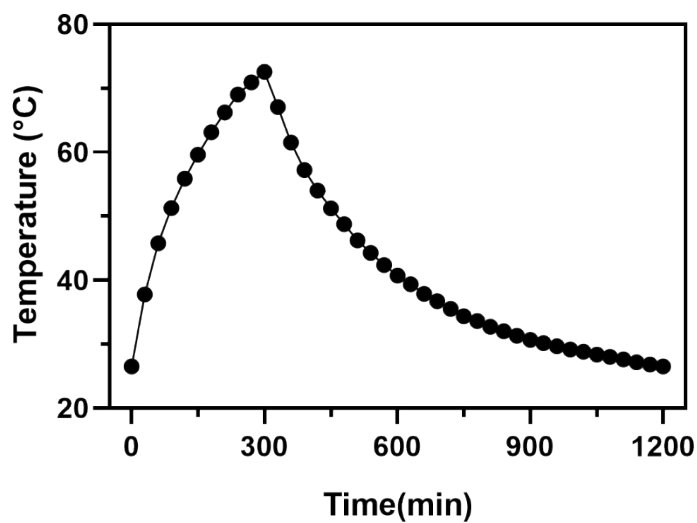


**Figure S2.** The temperature variation in Pd@Pt-PEG dispersions (200  $\mu\text{g/mL}$ ) under NIR laser irradiation (808 nm, 1  $\text{W/cm}^2$ ) for 300 s before shutting off the laser.

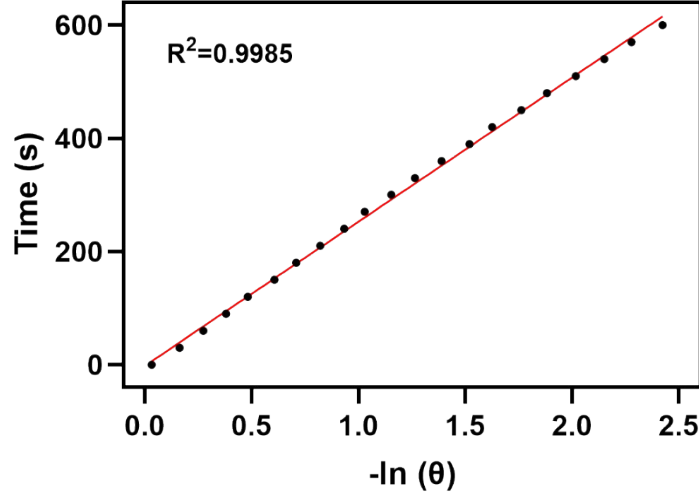


**Figure S3.** Negative natural logarithm of cooling time and temperature driving force gained from the cooling period data. The slope represents  $\tau_s = 254.69$  s.

The photothermal conversion efficiency ( $\eta$ ) of Pd@Pt-PEG can be calculated as following equations:

$$\eta = \frac{hS(T_{\max} - T_{\text{surr}}) - Q_{\text{dis}}}{I(1 - 10^{-A_{808}})} \times 100\% \quad (1)$$

In the equation above,  $h$  is the heat transfer coefficient;  $S$  is the irradiated area;  $T_{\max}$  is the equilibrium temperature;  $T_{\text{surr}}$  is ambient temperature of the surroundings;  $I$  is the laser power density ( $\text{W}/\text{cm}^2$ );  $Q_{\text{dis}}$  is the baseline energy input from the light absorption by the solvent;  $A_{808}$  is the absorbance of the Pd@Pt-PEG at 808 nm. Where  $h$  ( $\text{W}/\text{cm}^2 \cdot \text{K}$ ) means heat transfer coefficient,  $S$  ( $\text{cm}^2$ ) represents the surface area of the container. A dimensionless driving force temperature ( $\theta$ ) is introduced to calculate the value of  $hS$  using the following equations:

$$\theta = \frac{T - T_{\text{surr}}}{T_{\max} - T_{\text{surr}}} \quad (2)$$

$$t = -\tau_s \ln \theta \quad (3)$$

$$\tau_s = \frac{\sum m_i C_{p,i}}{hS} \quad (4)$$

Where  $m_i$  and  $C_{p,i}$  is the mass (1.0 g) and the thermal capacity (4.2 J/g) of deionized water used as a solvent,  $t$  is cooling time after irradiation, and  $\tau_s$  is the sample system time constant. On the basis of the above equation, the photothermal conversion of the Pd@Pt-PEG was determined to be about 74.5% under irradiation by an 808 nm laser.

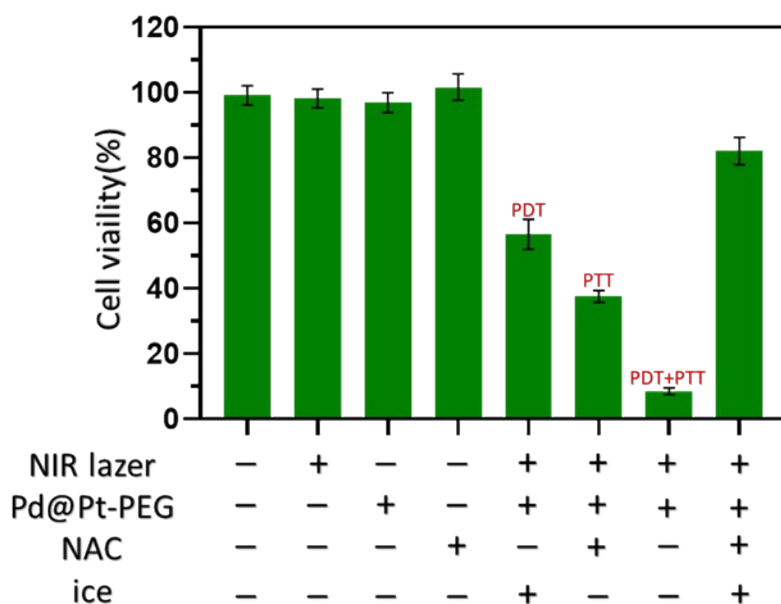


**Figure S4.** LM8 cell viabilities in different treatment groups.

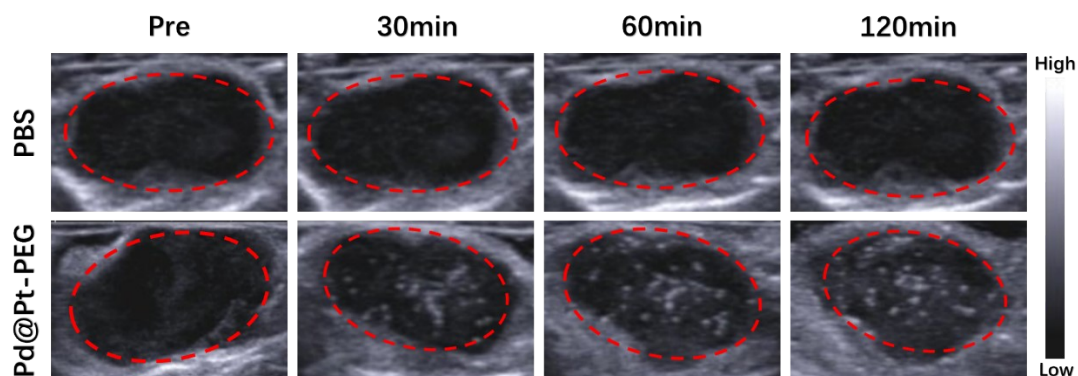


**Figure S5.** In vivo ultrasound images of tumor areas before and after intravenous administration of PBS (top) and Pd@Pt-PEG (bottom) at different times.

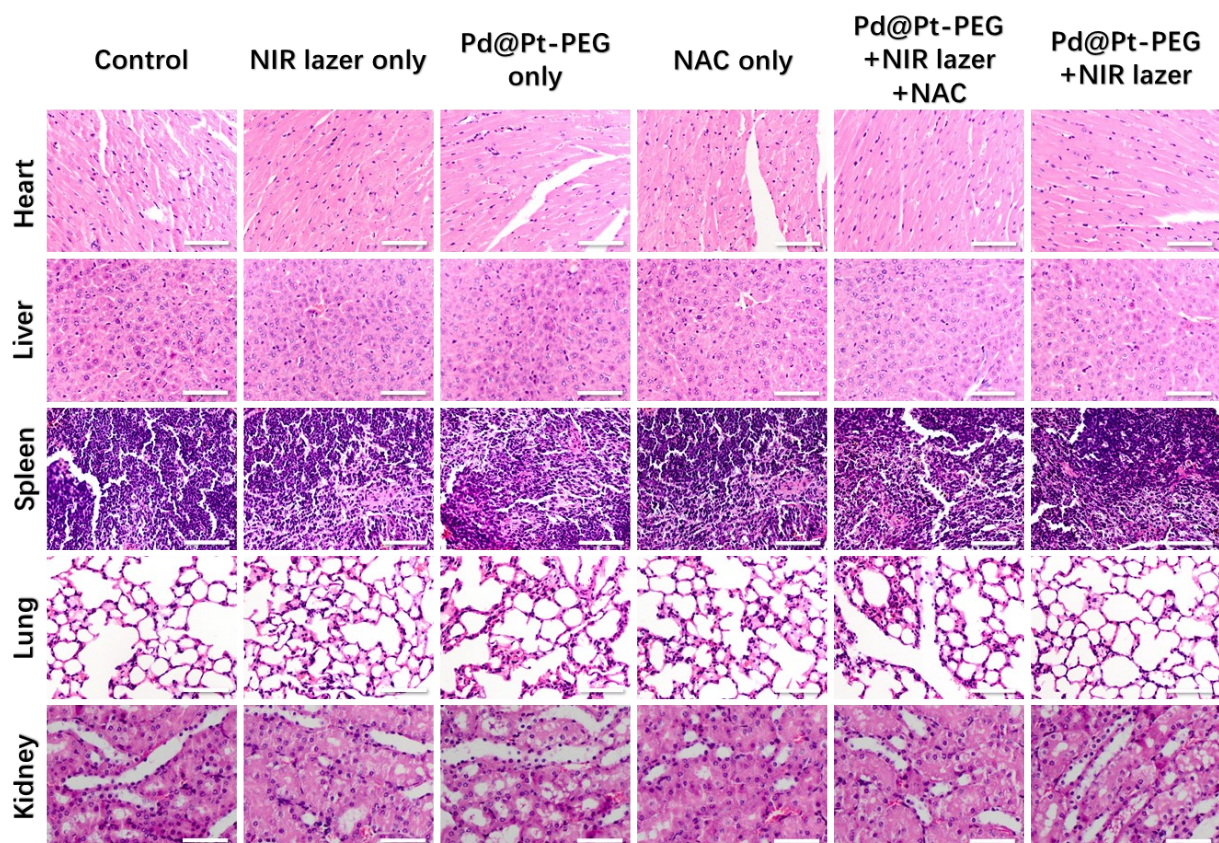


**Figure S6.** H&E staining of major organs excised from mice of different groups at 21th day. Scale bar: 100  $\mu$ m.



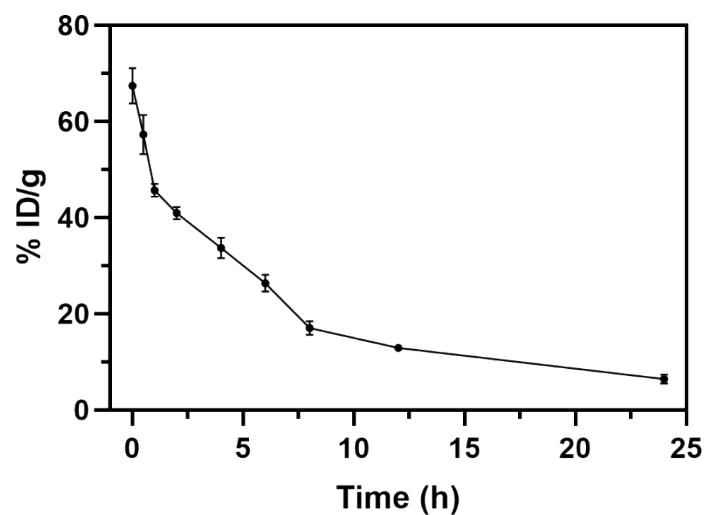


**Figure S7.** Blood levels of Pd@Pt-PEG after intravenous injection into mice as derived by detecting the percentage of Pd remaining in the blood at various time points.

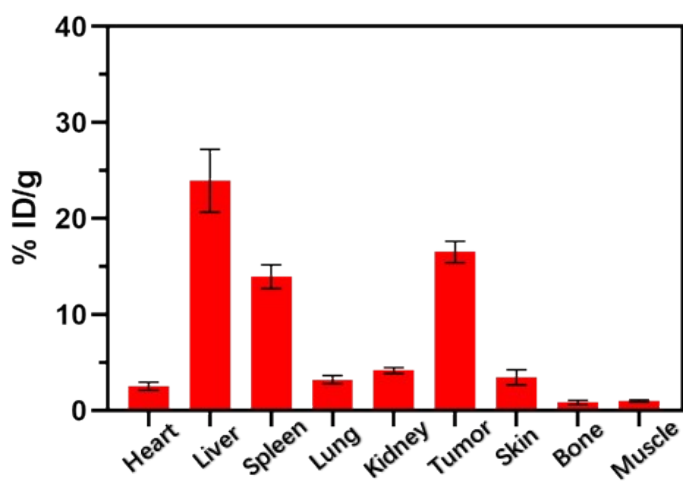


**Figure S8.** Biodistribution of Pd@Pt-PEG in major organs and the tumor detected at 24 post-injection.

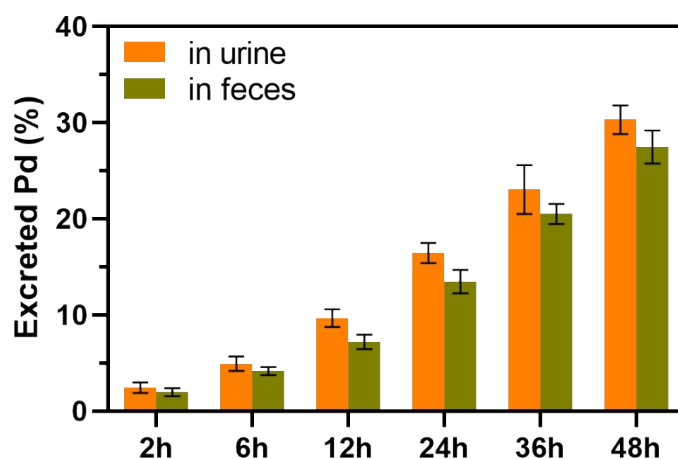


**Figure S9.** Accumulated Pd contents in urine and feces of mice after injection of Pd@Pt-PEG

collected at various time intervals.

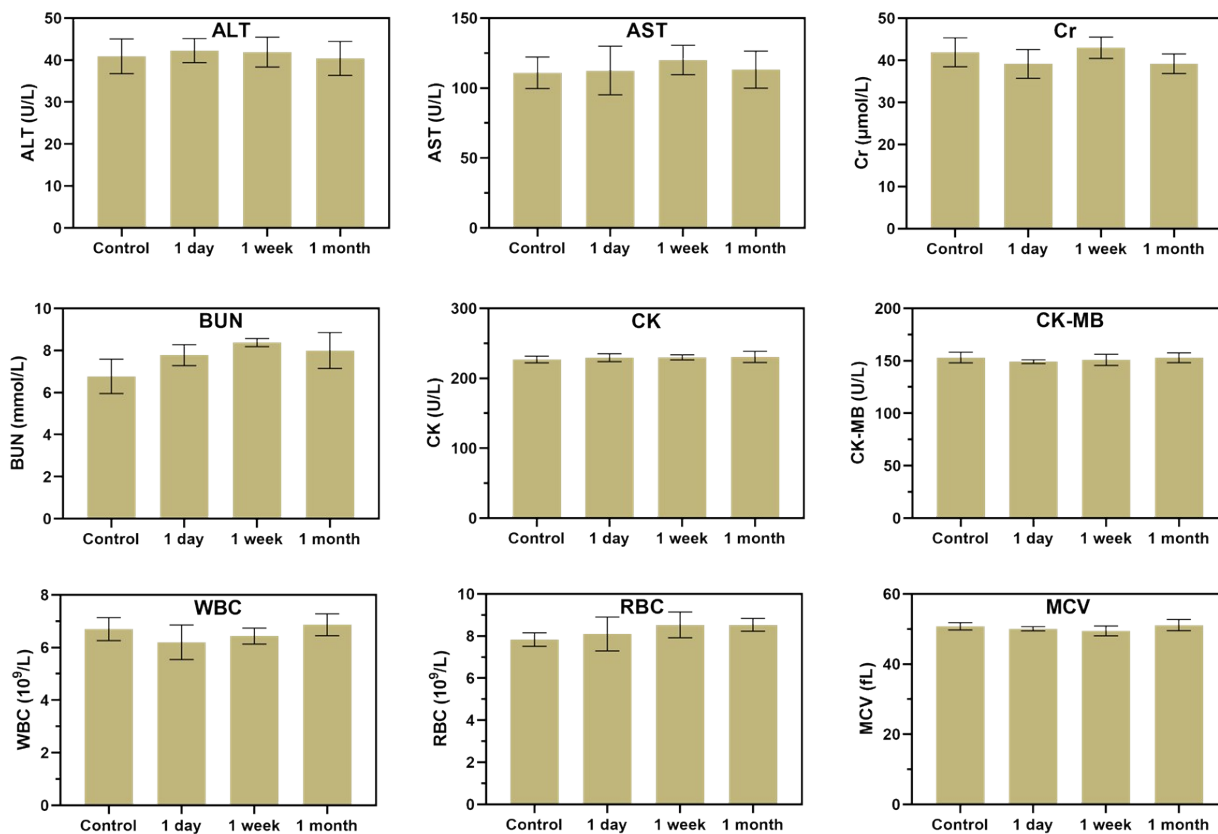


**Figure S10.** Serum biochemistry and hematology analysis of healthy mice after intravenously injected with Pd@Pt-PEG at 1st day, 7th day and 30th day.